# Electrostatic Potential Topography for Exploring Electronic Reorganizations in 1,3 Dipolar Cycloadditions

**P. Balanarayan, Ritwik Kavathekar, and Shridhar R. Gadre***

*Department of Chemistry, University of Pune, Pune 411 007, India*

*Received: November 3, 2006; In Final Form: January 30, 2007*

Topographical analysis of the molecular electrostatic potential (MESP) along a reaction path is employed for bringing out sequential electronic reorganizations for 1,3-dipolar cycloadditions of ethyne to fulminic acid as well as diazomethane. A simple and consistent set of rules for portraying electronic mechanisms of chemical reactions using the MESP topography is applied for this purpose. The MESP topography at each point on the concerted reaction path is associated with a classical electronic structure yielding a clear picture of the electronic reorganization along the reaction path.

## Introduction

1,3-dipolar cycloadditions (1,3-DCs) serve as an attractive route for the synthesis of five-membered heterocyclic compounds.[1] The ongoing debate relevant to 1,3-DCs deals with the microscopic nature of the electronic mechanism involved in the concerted reaction. 1,3-DCs have been a topic of constant interest since the debate between Huisgen's[1] depiction of a synchronous concerted route and Firestone's stepwise diradical pathway.[2] This debate was resolved by McDouall et al.[3] whose multiconfigurational self-consistent field calculations placed the concerted reaction to be energetically favorable than the nonconcerted diradical mechanism.

Given a concerted reaction path, what would be the nature of the arrows drawn in the mechanism for depicting the electronic reorganization? The two typical examples of 1,3-DCs, namely, the addition of ethyne (HCCH) to **(I)** fulminic acid (HCNO) and **(II)** diazomethane ($NNCH_2$) were examined by various groups for understanding the state and sequence of electronic reorganization along the concerted path. The current mechanisms for these 1,3-DCs are portrayed in Scheme 1.

Mechanism **I(b)** (Scheme 1) was proposed by Leroy et al.[4] based on the evolution of restricted Hartree−Fock Boys localized orbitals along the reaction path. This was supported by Karadkov et al.[5] using a spin-coupled valence bond approach for a synchronous reaction path generated by a complete active space self-consistent field (CASSCF) method. Mechanism **I(b)** involves an anticlockwise movement of electrons with the HCNO oxygen acting as a bond donor. Mechanism **I(a)** was proposed by Harcourt and Schultz[6] using valence bond (VB) theory at an STO-6G basis hinging upon the "apparent pentavalent nature" of the nitrogen in HCNO. Mechanism **I(c),** for which the oxygen acts as a bond acceptor, goes clockwise as depicted. Nguyen et al.[7] applied a configuration-interaction-localized molecular orbital-complete active space approach to come up with mechanism **I(c)**, with the addition being initiated by an electronic migration from oxygen to nitrogen of HCNO. This was again supported by an analysis of density functional theory (DFT)-based reactivity descriptors[8] and Fukui function indices[8] for electrophilic attack. The flow of electrons within $NNCH_2$ + HCCH (mechanisms **II(a)** and **II(b)**) are similar to mechanisms **I(b)** and **I(c)** of HCNO + HCCH, with the clockwise flow being proposed by Leroy and Sana[9] and the anticlockwise one given by Karadkov et al.[10]

**SCHEME 1: Electronic Mechanisms Proposed in the Literature for 1,3-DCs of (I) HCNO + HCCH and (II) $NNCH_2$ + HCCH; see refs 4−8 for details.**

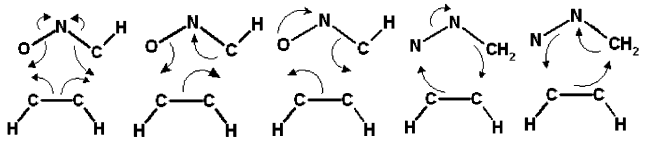

**I(a)** **I(b)** **I(c)** **II(a)** **II(b)**

One wonders how a given reaction could have multiple electronic mechanisms, all of which are apparently consistent within their own set of rules. All of the above mechanistic descriptions have been derived from wave function-based or orbital-based methods that have a certain amount of subjectivity due to the choice of orbitals or choice of method/wave function. An attractive way of circumventing this subjectivity is to rely on a function or descriptor that is unique and unambiguous in choice simultaneously relating to the electronic reorganization and other chemical concepts such as valence behavior and reactivity. One such analysis could be found in the catastrophes of the electron localization function (ELF) along the concerted reaction path of HCNO + HCCH as given by Silvi et al.[11] The electronic reorganization patterns emerge clearly from this ELF analysis and fall in line with mechanism **I(b)** (Scheme 1). Is an alternate stepwise description of this reaction that also bears a connection with classical chemical structures possible with the help of another scalar field?

In the current work, the electronic reorganizations during the 1,3-DC reactions, namely, **(I)** HCNO + HCCH and **(II)** $NNCH_2$ + HCCH are examined using the scalar field of molecular electrostatic potential (MESP),[12] which is a unique and experimentally derivable real quantity, given a nuclear arrangement and the corresponding electron density.[13] The ESP for a molecule with nuclear charges $\{Z_A\}$ at nuclear position vectors $\{\mathbf{R}_A\}$ and a continuous charge density $\rho(\mathbf{r})$ is given by

* To whom correspondence should be addressed. E-mail: gadre@chem.unipune.ernet.in.

10.1021/jp067247o CCC: $37.00 © 2007 American Chemical Society
Published on Web 03/16/2007

$$V(\mathbf{r}) = \sum_A \frac{Z_A}{|\mathbf{r} - \mathbf{R}_A|} - \int \frac{\rho(\mathbf{r}')}{|\mathbf{r} - \mathbf{r}'|} d^3r'$$

The value of this three-dimensional (3D) function has been closely connected with chemical concepts such as reactivity, Hammett constants,[14] aromaticity,[15] resonance and inductive effects,[15] weak intermolecular interactions,[16] and so forth. All of these works have utilized the condensed chemical information from MESP by analyzing its maximal and minimal characteristics given by its topography.[17] In view of this, the present work attempts an exploration of the electronic mechanisms of the 1,3-DC reactions by using MESP topography.

**Methodology and Theoretical Calculations.** The intrinsic reaction coordinate (IRC) paths were generated for HCNO + HCCH and $NNCH_2$ + HCCH with the Gaussian '03 suite of programs[18] using the DFT-Becke three-parameter exchange Lee, Yang, and Parr correlation functional (B3LYP) at the 6-311++G (2d, 2p) basis set. The activation barriers for the two reactions were found to be 15.74 and 17.44 kcal/mol, respectively. These are generally in agreement with the previously tabulated activation barriers.[19] The topography of MESP was mapped for various geometries along the IRC using the package INDPROP and visualized using the graphics package UNIVIS-2000.[20] The topographical analysis of the reactions involves three facets which have been described below.

**(i) Critical Points (CPs) of MESP.** The topography of any 3D function involves the identification and characterization of all its CPs, namely, minima (3, +3), saddles (3, −1) and (3, +1), and maxima (3, −3). The negative valued (3, +3) minima of ESP have been utilized as indicators of electron localization. The notation (R, S) is used for characterizing the CPs where R is the *rank* that denotes the number of nonzero eigenvalues and S is the *signature* (sum of the algebraic signs of the eigenvalues) of the Hessian matrix at the critical point given by $\mathbf{H}_{ij} = \partial^2 f/\partial x_i \partial x_j$ for a 3D function $f(x_1,x_2,x_3)$.[17] The set of CPs is found to satisfy the Poincaré−Hopf relation.[20−22] All *chemical notations* such as lone pairs, bonds, and $\pi$-bonds (aromatic, delocalized, and localized) have their topographical manifestations in MESP. The lone pairs and $\pi$-bonds have their interpretations via negative valued (3, +3) CPs. The positive valued (3, −1) CP in the internuclear region gives the manifestation of the bond; a positive valued (3, +1) CP is the manifestation of a ring. Negative and positive valued saddles may appear elsewhere in the scalar field connecting all of the other kinds of CPs. One of the main features of MESP which makes it very conducive for interpreting electronic mechanisms over the other scalar fields is that *non-nuclear maxima are absent*. Hence, the valence features are uniquely defined by the minima and the other kinds of CPs.

**(ii) Classification of Topographical Changes Based on Catastrophe Theory.** The changes in criticality have been mapped and isolated for the various points along the reaction path. They have been classified according to a catastrophe theoretical analysis.[23] Catastrophe theory deals with changes in the topography of a 3D function (a behavior space) with respect to a parametric (control space) change. In the reactions dealt with here, the *behavioral space* pertains to the MESP with the parametric *control space* being the external potential, the change in nuclear coordinates along the IRC. The types of basic catastrophes encountered for the 1,3-DCs are *fold*, *cusp*, and *butterfly*. This classification due René Thom[24] assigns a germinal behavior of a function $f(x) = x^3 + ax$ for that of a *fold* catastrophe with *a* being representative of the parametric change.

When the MESP or any 3D function encounters a fold *catastrophe*, the type of visible topographical change associated with it involves either the appearance or disappearance of 2 CPs. This 1D catastrophe would involve a coalescence (in the case of 2 CPs disappearing) of the maximal and minimal directions of two CPs. The *cusp* catastrophe in MESP or any 3D function shows a behavior similar to a function of the form $f(x) = x^4 + ax^2 + bx$ and the change involves 3 CPs.

**(iii) Asymptotics of MESP.** The asymptotics of MESP are defined[22] by the number of positive and negative island-like regions on a sphere with a very large radius. The positive regions on this surface have flux (with flux being defined as $\nabla V(\mathbf{r})$ and *not* the electric field $\mathbf{E} = -\nabla V(\mathbf{r})$) going into the sphere and thus are associated with *asymptotic minima*. The negative regions have flux going out of the sphere and are thus associated with *asymptotic maxima*. These regions manifest the $q/|r|$ behavior of MESP at large distances, where $q$ is a fractional charge associated with a region or regions. It is to be noted that MESP possesses distinctive asymptotic features for neutral systems since the Euler characteristic could be a number other than unity. However, for ELF, MED, or the Laplacian of MED, the Euler characteristic is always unity.

Some general guidelines for describing electronic mechanisms are derived from the above considerations and are listed below.

**A General Set of Rules for Depicting Electronic Mechanisms from the MESP Topography.** MESP shows predominant valence behavior, and all of these catastrophes manifest in the scalar field even for valence electron reorganizations indirectly related to bond breaking and formation. It is also to be noted that specific types of catastrophes such as a fold are related to ring formation and bond breaking in the case of MED. A particular type of catastrophe is not associated with a chemical event in the case of MESP. The chemical event as described by the arrows indicating electronic reorganization is explained in terms of and quantified by the MESP values at the CPs and their nature. The potential energy surface (PES)/IRC is divided into different structures via catastrophes, and the arrows (conventionally depicting a pair of electrons) are drawn by following the (3, +3) minima.

(1) Each structure on the IRC is characterized by the number of (3, +3), number of (3, +1), number of (3, −1), number of asymptotic maxima, and number of asymptotic minima. When a change in topography is observed along the reaction path, an arrow is drawn in the diagram. A subsequent structure is drawn after the occurrence of a catastrophe.

(2) The arrow is always drawn pointing in the direction of/following the shift of the (3, +3) CP of MESP. In the reactions studied here, the arrows are indicative of fold, cusp, and butterfly catastrophes.[23]

(3) Two (3, +3) minima with an intervening saddle correspond to two lone pairs. If along the reaction path the two minima and saddle merge into a single minimum and the MESP value of the new CP is more negative as compared with the preceding topography, then a "minus" **(−)** notation is assigned to the atom closest to the CPs. If the aforementioned process is accompanied by a more positive MESP value, then the change in topography corresponds to a loss of one of the lone pairs to a bonding process.

(4) A pair of negative valued (3, +3) minimum above and below the plane containing an internuclear axis is assigned a *double bond*. Examples for these could be observed in the case of the reactants studied in the current work and the cases of ethylene, butadiene, and so forth.

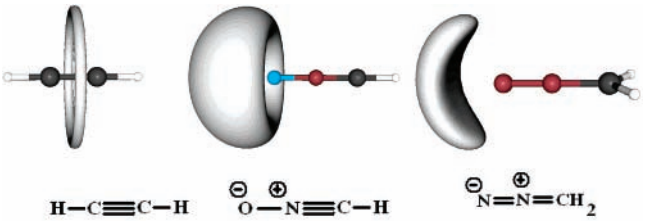


**Figure 1.** MESP characteristics for the reactants HCCH, HCNO, and $CH_2N_2$. The MESP iso-surface −0.028 au is plotted.

(5) A positive valued (3, −1) CP between two nuclei characterizes the bonding region. A high positive MESP valued CP is assigned a *bold line* denoting a strong bond. A low positive valued MESP CP is assigned a *dotted line* denoting a weak bond. In the case of ring formation, generally positive valued (3, −1) and (3, +1) CP are involved in a fold catastrophe.

(6) A conjugation or resonance of electrons over a ring is again associated[14,15] with (3, +3) CPs, with the accompanying (3, +1) saddles. This is exemplified by previous observations of the MESP topography of benzene in its equilibrium geometry having six negative valued (3, +3) CPs each over the carbons and six (3, +1) saddles (of a very similar function value) connecting them. Similar (3, +3) CPs have been observed for any aromatic ring system with substituents, although the number, positions, and function values at the CP's are different.

(7) It is observed that the difference between the number of asymptotic maxima and asymptotic minima is maintained constant along the reaction path. This has its explanation from the invariance of the Euler characteristic along a parametric change for a scalar field.

Thus, the topography of the MESP has a close association with classical structures and could be meaningfully exploited for following reaction paths.

## Results and Discussion

The topographical analysis of the MESP along the IRC is preceded by an analysis of the MESPs of the individual reactants. The MESP maps and the topographies of HCCH, HCNO, and $CH_2N_2$ are provided in Figure 1.

Acetylene has a degenerate ring of CPs at an MESP value of −0.0291 au. The degenerate ring that is stable to a geometrical distortion such as a symmetric stretching and unstable to an angular geometric change is reminiscent of the carbon−carbon triple bond. An angular distortion would in general result in lifting of the degeneracy of the ring of CPs, and this is indeed seen during the course of the reaction. HCNO has a negative valued (3, +1) CP on the $C_\infty$ axis with a degenerate ring of CPs near the oxygen at −0.0491 au. The bonding and the hypervalent nature of the nitrogen in HCNO has always been a point of discussion in the literature.[6,11] The nitrogen in HCNO remains immersed in a positive potential with no negative valued CP in its neighborhood. The nature of the MESP of HCNO thus enables an association of a classical structure in line with the generally known valencies, namely, $H-C\equiv N^+-O^-$. In contrast to HCNO, the terminal nitrogen in $CH_2N_2$ has two (3, +3) CPs at an MESP value of −0.0382 au. The $CH_2$ group of $CH_2N_2$ has two (3, +3) CPs above and below at an MESP value −0.0133 au. These CPs indicate that the double-bonded nature of the carbon, and hence a classical structure of $H_2C=N^+=N^-$, maybe assigned to diazomethane.

**(I) 1,3-DC HCNO + HCCH.** The reaction HCNO + HCCH is preceded by the formation of a pre-reaction complex (PRC) with an interaction energy of −1.77 kcal/mol. The PRC involves a weak interaction between the ethyne hydrogen and one of the lone pairs of oxygen resulting in an angular weak complex. The topography of HCNO and HCCH with respect to the number of CPs does not change in the PRC, except for the degeneracy being lifted for HCCH and a more negative potential appearing in its neighborhood. The formation of the PRC is seen to make the MESP near oxygen less negative. The topography indeed qualitatively and quantitatively shows that there is no major electronic reorganization and that the prevalent interactions are predominantly electrostatic. The reactants have just been prepared for the major shifts, and this occurs at a reaction coordinate of −1.49978 amu/bohr from the transition state (TS) taken as 0.0 on the reaction coordinate.

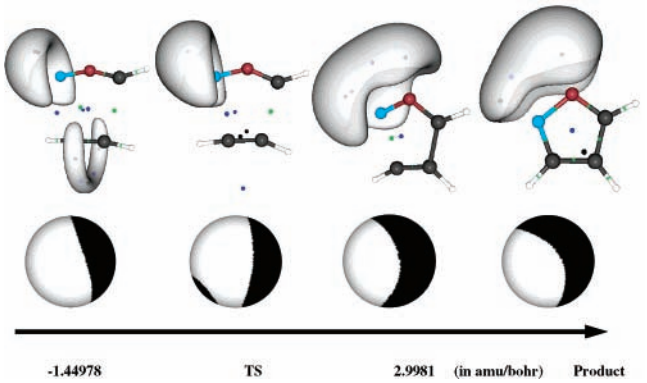


**Figure 2.** MESP topography (black (3,+3), blue (3, +1), and green (3, −1) dots for CPs) and isosurfaces (−0.028 au) along the reaction path. The asymptotics are depicted on a sphere of radius 20 au centered at the center of mass, with the black and white regions denoting positive and negative MESP, respectively.

The first major electronic reorganization manifests itself as a butterfly catastrophe, where the behavior of the potential below the CC triple bond of HCCH is similar to that of a function of the form $f(x) = x^6 + ax^4 + bx^3 + cx^2 + dx$. This is followed by yet another change in criticality in the same region, and the result is two negative valued (3, +3) CPs at −0.0322 au MESP value, which are reminiscent of a C═C. The topography attained by HCCH at this point in the reaction is similar to that of ethylene, which has two (3, +3) CPs perpendicular to the plane in which the double bond lies. A concurrent occurrence is the increase in the positive nature of the (3, −1) CP connecting the carbons of HCCH and HCNO. All of these point toward an electronic shift from acetylene to a strong bond formation between the carbons. The MESP values and the nature of the CPs predominantly evolving during the course of the reaction are reported in Table 1.

After the first major electronic reorganization, the topography of the TS indicates a noncyclic structure and a positive potential is observed in the vicinity of the terminal carbon of HCCH. The next major electronic reorganization is seen in terms of the appearance of a (3, +3) CP above nitrogen, and at the same time, there is a decrease in the MESP value of the (3, −1) CP of the CN bond. This indicates a weakening of the bond and a shift of electrons from the CN bond to the nitrogen.

The topography-based mechanism so far conforms to arrows moving in an anticlockwise direction as put forth earlier by Leroy et al.[4] and Karadkov et al.[5] A pictorial description of this is displayed in Figure 2 that includes the MESP topography, isosurfaces, and asymptotics which form the basis of the envisaged reaction mechanism.

The terminal carbon of the noncyclic TS is immersed in a positive potential and structures after the TS show a percolation

**TABLE 1: MESP Values in atomic units and the Nature of CPs along the IRC for Reaction (I) HCNO + HCCH at the B3LYP/6-311++G(2d,2p) Level of Theory[a]**

| reaction coordinate (amu/bohr) | CC of HCCH | CC (3, -1) | O minima | N minimum | OC bond |
|---|---|---|---|---|---|
| −1.449778 | −0.0326(+3) | +0.0880 | −0.0484 (2) | absent | |
| −1.39786 | −0.0322(+1) | +0.1674 | −0.0486 (2) | absent | |
| 0.00000 **(TS)** | −0.0255(+1) | +0.1874 | −0.0533 (1) | absent | no CP |
| 0.99823 | +0.0019 (+1) | +1.2102 | −0.0566 (1) | absent | |
| 1.99817 | CP vanishes | +1.3468 | −0.0577 (1) | −0.04168 | |
| 2.99811 | absent | +1.4572 | −0.0571 (2) | −0.05585 | +0.1650 |
| 2.99798 | absent | +1.4783 | −0.0549 (2) | −0.06575 | +0.2617 |
| 4.99790 | absent | +1.4863 | −0.0521 (2) | −0.07277 | +0.4302 |
| product | | +1.5068 | −0.0422 (1) | −0.07961 | +1.2378 |

[a] The number of CPs wherever relevant are given in parentheses. See text for details.

**SCHEME 2: MESP Topography Derived Reaction Mechanism for (I) HCNO + HCCH 1,3-DC.**

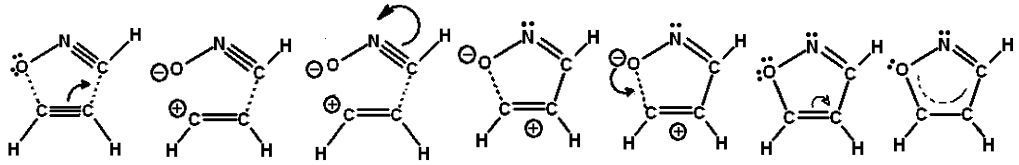

**(i) (ii) TS (iii) (iv) (v) (vi) Product(vii)**

of this positive potential toward the other connected carbons. This is reminiscent of the positive charge going into conjugation in the plane of the ring. The final electronic reorganization that occurs is the coalescence of two (3, +3) minima and a (3, +1) saddle above oxygen to give a single minimum. This could be interpreted as one of the lone pairs going into conjugation in the ring following the previously mentioned percolation of positive potential. The final topography of the product has two (3, +3) minima over the carbon at the vertex of the product as a result of a fold catastrophe.

An examination of the asymptotics of the MESP (Figure 2) confirms that the *electron flow* is always toward the positive potential. The asymptotic behavior of the MESP up to and beyond the TS is indicative of a *waxing* and *waning* of the positive potential. When a point on the IRC has a positive potential region, the electron reorganization is seen to occur toward that region at the subsequent point. The positive potential grows to a maximum to a point beyond the TS. Thereafter, the major electronic reorganization occurs in the form of a resonance of electrons into the ring bringing back a percolation of the negative potential region.

The product of the reaction indeed possesses an interesting topography, with the salient features being two (3, +3) CPs (at −0.015 au MESP value) above and below the plane of the ring over the second carbon of HCCH. These CPs are the result of two fold catastrophes on either side of the ring. It is also seen that at a preceding point the oxygen minima and saddle have merged into a single minimum via a cusp catastrophe. This is indicative of the oxygen losing one of its lone pairs. The appearance of aforementioned minima suggests an unconventional electronic structure for the product that has been depicted in Scheme 2 with the dotted curve indicating electron delocalization over the two carbons and oxygen. The following depiction for the product is similar to the MESP topography-based formulas previously suggested by Suresh et al.[15] All of the above-described phenomena are summarized in Scheme 2, with the complete mechanism being given and associated with classical structures.

In comparison with the ELF mechanism suggested by Polo et al.[11] at a gross level, the MESP mechanism also predicts an anticlockwise electronic reorganization for the reaction. However, there are certain subtle differences in the step-by-step mechanism. The ELF mechanism shows the nitrogen developing a lone pair character in an early stage of the concerted reaction, whereas in the MESP mechanism this occurs only at a later stage. Although such microscopic differences do not have substantial importance in the case of concerted reactions, there are some further important insights gained via the MESP mechanism, with the major difference being topographical evidence for the conjugated nature of the product, finally giving a depiction as seen in Scheme 2 **(vii)**.

**(II) 1,3-DC $NNCH_2$ + HCCH.** Starting with an MESP topography-derived classical structure of $H_2C{=}N^+{=}N^-$ to ethyne, a PRC is formed with an interaction energy of −1.15 kcal/mol. The PRC is similar to that for reaction **(I)** with the terminal nitrogen weakly interacting with an ethyne hydrogen. The major step of electronic reorganization for this reaction starts off at a reaction coordinate of −1.49724 amu/bohr, with the topographical manifestation being two fold catastrophes, where one is occurring with the CPs concerned with the double-bonded carbon of diazomethane and the other occurring with the beginning of a bond formation between the ethyne carbon and diazomethane carbon. The catastrophes indicate the loss of the $sp^2$ nature of the diazomethane carbon. The next major electronic shift (occurring at −0.7563 amu/bohr, very close to the TS) is again seen in terms of a butterfly catastrophe. This is followed by a cusp catastrophe occurring with the CPs concerned with the CC triple bond becoming double bonded as per the MESP topography at the TS.

The TS has been depicted in Scheme 3 as a cyclic structure, thus differing from the TS of reaction (**I**). After the TS, the only major reorganization is the appearance of a negative minimum near the nitrogen that was previously in a positive potential. The number of catastrophes occurring for this reaction is less in comparison with reaction **(I)**. The asymptotics of the MESP further support the anticlockwise direction arrows depicted in Scheme 3. The details of the MESP topography and catastrophes have been given in the Supporting Information. The product for the reaction has a topography that indicates

**SCHEME 3: MESP Topography-driven Reaction Mechanism for (II) $NNCH_2$ + HCCH 1,3-DC.**

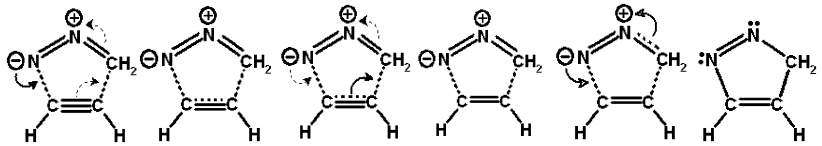

**(i) (ii) TS(iii) (iv) (v) (vi)**

localized double bonds which are not involved in resonance as can be seen in the case of reaction **(I)**.

## Concluding Remarks

Use of electron-density-based scalar fields offers an attractive alternative for following reaction pathways. ELF-based studies[11] are seen to be successful for a topography-based description of the reactions probed in this work. The use of MESP topography along a reaction path offers a direct correspondence with electronic shifts and the arrows drawn in electronic mechanisms. This has been tested for the two prototypic 1,3-DC reactions, and the electronic mechanisms for the reactions have been depicted. The electrostatic mechanism for the 1,3-DC of HCNO + HCCH is in agreement with mechanism **I(b)**. The MESP is a one-electron property which is rather insensitive to correlation, when a good (at least polarization + double-$\zeta$) basis set is used. Thus, the essential features of the electronic mechanism could be captured by Hartree−Fock or B3LYP quality MESPs. The subjectivity involved in the use of orbitals is thus largely eliminated by ELF as well as MESP.

Yet another advantage that MESP has in elucidating reaction mechanisms is the very nature of the negativity of the function being very close to classical concepts of valence, lone pairs, and so forth. In comparison, the topography of the molecular electron density (MED) as a 3D function is mainly associated with just criticalities along bonding directions. The electron density lacks details in the subtle changes of valence electron distribution. Laplacian of MED however does possess certain features which could be attributed to valence phenomena, and this has been used before in an early pioneering work on cycloaddition reaction pathways.[25] The ELF which is derived from the density does have valence-related maxima and bonding maxima, but a microscopic interpretation of the process of electronic reorganization warrants an integration over the basins of these maxima as well and offers quantitative information.

Just the asymptotic behavior of MESP enables further insights into reaction mechanisms as illustrated in the case of reaction **(I)**. In contrast to ELF which asymptotically dies off as a maximum and MED which dies off asymptotically as a minimum, MESP possesses asymptotic maxima as well as minima. The asymptotic maxima refer to zeroes approached from the negative side while the minima refer to zeroes approached from the positive side. The asymptotic behavior is particularly insensitive to basis set and correlation effects.

The efficacy of MESP topography in elucidating the electronic mechanisms of concerted reactions revealed via the analysis of two 1,3-DCs, namely, HCNO + HCCH and $NNCH_2$ + HCCH, also circumvents the subjectivity involved in a wave-function-based analysis. The reaction mechanisms derived from MESP topography find a further quantitative footing using catastrophe theory. In the particular case of the 1,3-DCs wherein the literature finds multiple mechanisms from wave-function-based methods, the MESP topography-derived mechanism gives a single consistent one. It is to be noted that a one-electron property such as MESP is fairly insensitive to correlation effects. When the MESP is evaluated using the wave functions employed for formulating the multiple mechanisms **I(a)**, **I(b)**, and **I(c)**, and the topography along the reaction path, one would arrive at a single reaction mechanism. In contrast to other scalar fields such as MED, MESP topography has a close connection with the valence electron behavior through a topographical manifestation of lone pairs and $\pi$-bonds. The derived reaction mechanisms also connect well with the classical chemical concepts. It is hoped that the present study gives impetus to the use of MESP as an effective tool for understanding and unearthing organic reaction mechanisms along with other scalar fields such as ELF which have been employed before.

**Acknowledgment.** P.B. thanks the Council of Scientific and Industrial Research (CSIR), New Delhi, and Center for Development of Advanced Computing (C-DAC), Pune, for a research fellowship.

**Supporting Information Available:** Tables of lists of catastrophes and topographies of MESP. This material is available free of charge via the Internet at http://pubs.acs.org.

## References and Notes

(1) Huisgen, R. *Angew. Chem., Int. Ed. Eng.* **1963**, *2*, 633. Huisgen, R. *J. Org. Chem.* **1976**, *41*, 403.

(2) Firestone, R. *J. Org. Chem.* **1968**, *33*, 2285. Firestone, R. *Tetrahedron* **1977**, *33*, 3009.

(3) McDouall, J. J. W.; Robb, M. A.; Niazi, U.; Bernardi, F.; Schlegel, H. B. *J. Am. Chem. Soc.* **1987**, *109*, 4642.

(4) Leroy, G; Sana, M.; Burke, L. A.; Nguyen, M. T. In *Quantum Theory of Chemical Reactions*; Daudel, R., et al.; Eds.; D. Reidel: Amsterdam, The Netherlands, 1979.

(5) (a) Karadkov, P. B.; Cooper, D. L.; Gerratt, J. *Theor. Chem. Acc.* **1998**, *100*, 222. (b) Karadkov, P. B.; Cooper, D. L.; Gerratt, J. *J. Am. Chem. Soc.* **1998**, *120*, 3975.

(6) Harcourt, R. D.; Schultz, A. *J. Phys. Chem. A* **2000**, *104*, 6510.

(7) Nguyen, M. T.; Chandra, A. K.; Uchimaru, T.; Sakai, S. *J. Phys. Chem. A* **2001**, *105*, 10943. Sakata, K. *J. Phys. Chem. A* **2000**, *104*, 10001.

(8) Chandra, A. K.; Nguyen, M. T. *J. Phys. Chem. A* **1998**, *102*, 6181; *J. Comput. Chem.* **1998**, *19*, 195; *J. Chem. Soc., Perkin Trans. 2* **1997**, 1415.

(9) Sana, M.; Leroy, G.; Dive, G.; Nguyen, M. T. *J. Mol. Struct. (THEOCHEM)* **1982**, *89*, 142.

(10) Blavins, J. J.; Karadkov, P. B.; Cooper, D. L. *J. Phys. Chem. A* **2003**, *107*, 2548.

(11) Polo, V.; Andres, J.; Castillo, R.; Berski, S.; Silvi, B. *Chem.−Eur. J.* **2004**, *10*, 5165.

(12) For a detailed review on molecular electrostatics, see Gadre, S. R.; Shirsat, R. N. *Electrostatics of Atoms and Molecules*; Universities Press: Hyderabad, India, 2000.

(13) Jackson, J. D. *Classical Electromagnetism*; Wiley Eastern: New Delhi, India, 1978.

(14) Suresh, C. H.; Gadre, S. R. *J. Am. Chem. Soc.* **1998**, *120*, 7049.

(15) Suresh, C. H.; Gadre, S. R. *J. Org. Chem.* **1999**, *64*, 2505.

(16) Gadre, S. R.; Bhadane, P. K.; Pundlik, S. S.; Pingale, S. S. In *Molecular Electrostic Potential: Concepts and Applications*; Murray, J., Sen, K. D., Eds.; Elsevier: Amsterdam, The Netherlands, 1996.

(17) Gadre, S. R. In *Computational Chemistry: Reviews of Current Trends*; Leszczynski, J., Ed.; World Scientific: Singapore, 2000**;** Vol. 4, p 1.

(18) Frisch, M. J.; et al. *GAUSSIAN 03*, Gaussian Inc.: Pittsburgh, PA, 2003.

(19) Nguyen, M. T.; Chandra, A. K.; Sakai, S.; Morokuma, K. *J. Org. Chem.* **1999**, *64*, 65.

(20) INDPROP and UNIVIS-2000, the molecular properties calculation and visualization package, see Bapat, S. V.; Shirsat, R. N.; Gadre, S. R. *Chem. Phys. Lett.* **1992**, *200*, 373. Limaye, A. C.; Gadre, S. R. *Curr. Sci. (India)* **2001**, *80*, 1296. Balanarayan, P.; Gadre, S. R. *J. Chem. Phys.* **2003**, *119*, 5037.

(21) Bader, R. F. W. *Atoms in Molecules: A Quantum Theory*; Oxford University Press: Oxford, U.K., 1990.

(22) Leboeuf, M.; Köster, A. M.; Jug, K.; Salahub, D. R. *J. Chem. Phys.* **1999**, *111*, 4893.

(23) (a) Poston, T.; Stewart, I. N. *Taylor Expansion and Catastrophes*; Pitman Publishing, London, 1976. (b) Saunders, P. T. *An Introduction to Catastrophe Theory*; Cambridge University Press: 1980.

(24) Thom, R. In *Structural Stability and Morphogenesis*; Benjamin: Reading, 1975.

(25) Gatti, C.; Barzghi, M.; Bonati, L.; Pitea, D. Quantum Chemistry—Basic Aspects, Actual Trends. In *Studies in Physical and Theoretical Chemistry*; Elsevier: 1989; Vol. 62, p 401.